ACADEMIC PRESS

Available online at www.sciencedirect.com
SCIENCE DIRECT®

NeuroImage

NeuroImage 19 (2003) 1812–1819

www.elsevier.com/locate/ynimg

Positron emission tomography during transcranial magnetic stimulation does not require μ-metal shielding

Jae Sung Lee,[a] Shalini Narayana,[b] Jack Lancaster,[b] Paul Jerabek,[b] Dong Soo Lee,[a] and Peter Fox[b,*]

[a] *Department of Nuclear Medicine, Seoul National University College of Medicine, Seoul 110-744, Korea*
[b] *Research Imaging Center, University of Texas Health Science Center at San Antonio, 7703 Floyd Curl Drive, San Antonio, TX 78284-6240, USA*

Received 13 June 2002; revised 3 April 2003; accepted 7 May 2003

Abstract

Recording brain activity using positron emission tomography (PET) during the stimulation of different parts of the brain by transcranial magnetic stimulation (TMS) permits the mapping of neural connections in the living human brain. However, controversy remains regarding the need for μ-metal shielding of the PET scanner during magnetic stimulation. The aim of this study was to test the effects of magnetic fields generated by TMS on PET data acquisition. With TMS-on and -off in the PET field of view, transmission scans with a $^{68}Ge/^{68}Ga$ pin source and emission scans with an uniform phantom filled with water and ^{18}F were acquired. The frequency and intensity of stimulation were set at 3–5 Hz and 70–80% of the maximum output of the stimulator, respectively. The TMS coil was placed at several locations inside the PET gantry, and the main field direction of the TMS coil was varied between parallel and perpendicular orientation to the scanner's axis. Qualitative and quantitative evaluation of the sinograms of transmission PET scans and reconstructed emission images indicated no measurable differences between TMS-on and -off and post-TMS conditions for any position or orientation. The long distance between the TMS coil and the detector block in the PET scanner, as well as the rapid reduction of the magnetic field with distance (3% of maximum field at 10 cm, in air), could explain the lack of TMS interference. The brief duration ($\sim$250 μs) of the TMS pulses relative to the total PET acquisition time would also explain the lack of TMS effects. The lack of TMS effects on the PET scanner, as well as PET imaging without any shielding, has been reported by other laboratories.

Introduction

Transcranial magnetic stimulation (TMS) is a noninvasive way of inducing a current flow in tissues and leads to the excitation of neurons (Barker et al., 1985). Recording TMS-induced neuronal activity by imaging methods during the magnetic stimulation of different parts of the brain permits the assessment of cortical excitability and the mapping of direct neural connections in the living human brain (Fox et al., 1997). Among the various techniques that allow us to measure the local and remote responses in the cerebral cortex stimulated by TMS, positron emission tomography (PET) has been the most widely used. PET allows the regional cerebral blood flow change to be measured using ^{15}O-labeled water as a tracer (Fox et al., 1997; Paus et al., 1997, 1998).

There are, however, several technical issues to be resolved in PET imaging studies during stimulation by TMS (Paus, 1999; Lee et al., 2000). The possible effects of the TMS magnetic fields on the operation of the photomultipliers (PMTs) used in the PET scanner are one such issue which is important. However, the topic of effects of magnetic stimulation on the PET scanner remains controversial. Fox et al. (1997) imaged a line phantom of ^{18}F to determine whether the magnetic field produced by TMS produces an artifact in PET images. No differences between the TMS-on and TMS-off conditions were reported by visual comparison of the reconstructed image by subtraction of the images or by transformation to statistical parametric images of *z*-scores (Fox et al., 1997). The lack of effects seen by Fox et al. was attributed to the low frequency (1 Hz) of magnetic

* Corresponding author. Fax: +1-210-567-8103.
E-mail address: fox@uthscsa.edu (P. Fox).

1053-8119/03/$ – see front matter © 2003 Elsevier Inc. All rights reserved.
doi:10.1016/S1053-8119(03)00239-8

stimulation used in the experiment and to the orientation of the TMS coil (Paus et al., 1998). The TMS coil was arranged such that the maximum *B* field was parallel to the scanner's axis and thereby minimized the possible interference between the magnetic field and PMTs. Thompson et al. (1998) reported that the magnetic fields associated with TMS disturbed the operation of a PMT detector assembly (Thompson et al., 1998). Their work was performed only on a pair of detectors. In the absence of μ-metal shielding, TMS induced degradation in the ability to identify the crystal in which the γ rays from positron annihilation are detected was demonstrated. Based on these findings, μ-metal shielding of the PET scanners during TMS has been recommended. However, the effect of TMS within a PET scanner has not been studied, and the effects on PET imaging during TMS without μ-metal shielding have not been demonstrated. Paus et al. (1997) did demonstrate a 22% loss in coincidence counts due to shielding of the PET scanner with μ-metal. Since the μ-metal shielding is put in place only during TMS/PET studies, a blank scan must be reacquired each time. There is also an increase in the scatter component due to the μ-metal shielding. Thus, μ-metal shielding during TMS degrades PET image quality, while its beneficial effects are yet to be demonstrated. To settle this controversy, we performed extensive TMS/PET experiments at higher stimulation frequencies and various coil orientations and distances from the PET gantry. These data were analyzed to identify possible effects of the magnetic field of TMS on the quality of PET data. We also surveyed the TMS/PET protocols of other TMS laboratories. We obtained personal communications from Bruce Weber at the University Hospital, Zurich, and Margaret Daube-Witherspoon at the University of Pennsylvania, who have also investigated the effects of TMS on an intact PET scanner in a manner similar to our experiments.

Materials and methods

A Cadwell high speed magnetic stimulator (Kennewick, WA, USA) and a water-cooled B-shape coil were used for all experiments. The stimulator produces a biphasic pulse with a total duration of about 250 μs and is capable of delivering pulses at a rate of up to 25 Hz with no reduction in intensity. The point of maximum field is under the central windings of the B-shape coil. A neurosurgical robot, NeuroMate, with a modified tool-holding mechanism, held the B-shape coil immobile for the duration of the experiment, providing consistency in terms of both the location and the orientation of the electromagnetic field (Narayana et al., 2000).

All data were acquired with a GE/Scanditronix whole-body PC4096 PET scanner (8 rings housing 4096 BGO detectors; pixel spacing = 2.0 mm; in-plane resolution = 5.5 mm FWHM; axial resolution = 6.0 mm FWHM; scan planes = 15, *z*-axis field of view = 10 cm, true sensitivity = 4500 cps/μCi/mL). The detector ring diameter of this scanner is 101 cm and the patient port diameter of the gantry is 57 cm.

Experiment I

To test the effect of the TMS-induced magnetic field on PET data acquisition in various orientations of the TMS coil and distances from the PET gantry, transmission PET images with a ^{68}Ge/^{68}Ga pin source were acquired under TMS-on and TMS-off conditions in the PET field of view. The frequency and intensity of stimulation were set at 3 Hz and 70% of the maximum output of the stimulator, respectively, as these settings were the most routinely used protocols in our institution (Research Imaging Center, UTHSCSA). Routinely, TMS experiments are performed with intensity settings near a subject's motor threshold ($\pm$10%). The average motor threshold from TMS studies (n = 48) in this institution was 62.8% Cadwell output. Therefore, we chose 110% of the average motor threshold, which is $\sim$70% of Cadwell output, for the intensity. Regional cerebral blood flow (rCBF) (as measured by ^{15}O-water-PET) during TMS is the most commonly measured parameter with PET at our institution. TMS delivered at 3 Hz yields good single subject CBF responses (Tandon et al., 2001; Narayana et al., 2002). The arrangement of the maximum field of the TMS coil was varied between parallel and perpendicular orientations to the scanner's axis (Fig. 1A and B). The distance between the point on the TMS coil where the magnetic field is maximum and the patient port edge of the PET gantry was varied from the minimum achievable distance (6 cm in parallel position and 2 cm in the perpendicular position, the position at which the edges of the coil touched the patient port edge of the PET gantry) to 21 cm.

For each orientation and distance, a transmission scan was acquired for 9 min while the TMS was turned off (TMS-off). After performing the TMS-off scan, 3-min transmission scans were acquired three times while the 3-Hz TMS was turned on (TMS-on) and summed to make 9-min images. This was done to prevent overheating of the TMS coil and overload of the magnetic stimulator power supply (Fig. 2A). A total of 1620 TMS pulses (3 Hz $\times$ 180 s $\times$ 3 scans) were delivered during the 9-min TMS-on condition. The Cadwell water-cooled TMS coil can discharge at high rates (up to 25 Hz). In almost all studies where TMS is used, prolonged TMS is applied at rates $\leq$1 Hz, while the high rate TMS ($\geq$5 Hz) is applied for periods of less than a minute (Pascual-Leone and Walsh, 2002). In our experience, the power supply and diodes in the Cadwell fail when the unit is operated at rates greater than 5 Hz and intensities greater 70% for periods longer than 3 min. To avoid this damage, we limit the use of Cadwell for rates of $\geq$5 Hz to durations less than 3 min. Therefore, we acquired the transmission images during the TMS-on condition in 3-min blocks. We waited for more than 10 min between PET scans for each orientation and distance to imitate a typical ^{15}O-

water-PET study and to prevent possible posteffects of the magnetic field on the next TMS-off scan.

Experiment II

Since we could not find any measurable difference between the TMS-on and -off conditions in the first experiment, we performed the same experiment using higher frequency and intensity. We increased the frequency of the magnetic stimulation to 5 Hz and intensity to 80% of maximum output. TMS during each scan session was reduced to 1 min, but by increasing the number of scan sessions, the total duration of TMS remained at 9 min (same as experiment I). The choice of these parameters was based on TMS/PET paradigms used at this institution and the limitation of the Cadwell stimulator (see under experiment I). Arrangement of the TMS coil was varied between parallel and perpendicular orientations (Fig. 1A and B). The TMS coil was positioned as close as possible in both orientations (6 cm in the parallel position and 2 cm in the perpendicular position from the patient port edge of the PET gantry).

In each orientation, nine 3-min transmission PET scans were performed. In each 3-min session, 1-min transmission scans with TMS-off, TMS-on, and post-TMS (post-TMS immediately after TMS-on) were acquired in sequence (Fig. 2B). A total of 2700 TMS pulses (5 Hz $\times$ 60 s $\times$ 9 scans) were delivered during the 9-min TMS-on condition. The sinograms acquired under the same conditions were summed to construct 9-min images, in the same manner as in the first experiment.

Experiment III

This experiment was performed in the same way as experiment II except that we acquired emission scans rather than transmission scans. Emission scans of a cylindrical uniform phantom filled with water and ^{18}F (0.39 μCi/mL concentration) were acquired. The arrangement of the TMS coil was also varied between the parallel and perpendicular orientations (Fig. 1C and D). The TMS coil was positioned as in the second experiment. Since ^{15}O-water studies are typically acquired for 1 min, we acquired emission scans of 1-min duration, repeated five times for each condition. Emission images were reconstructed as 128 $\times$ 128 $\times$ 15 matrices after attenuation correction by means of a filtered back-projection algorithm employing a Hanning filter with a cutoff frequency of 5 cycles/pixel.

Data analysis

Sinograms of transmission scans acquired in experiments I and II and their subtraction images were visually inspected. In addition, surface plots of the sinograms and subtraction images were made to allow detailed inspection of the 2D images. Sinograms are very sensitive variations in PMT output, and each detector has a distinct representation in a sinogram. Therefore, sinograms are more sensitive indicators of count difference than the reconstructed attenuation map. The reconstruction process propagates the error and noise in the sinogram and degrades the spatial resolution. Therefore, we chose to examine the sinograms of transmission and emission scans.

Since the reconstructed images of emission scans obtained in experiment III were rather noisy, they were smoothed by convolution using an isotropic Gaussian kernel with 16 mm FWHM after ^{18}F decay correction. Smoothing of images with the Gaussian kernel is a typical procedure used when analyzing images acquired with a short acquisition time as in brain activation studies using the ^{15}O-water protocol. Smoothed images were examined in two other ways. First, smoothed images obtained under the same conditions were summed to make 5-min images, and the summed images were examined in the same manner as the sinograms of transmission scans. Second, the statistically significant difference in voxel count between the images obtained under the three conditions (TMS-off, TMS-on, and post-TMS) was estimated at every voxel based on the general linear model using the SPM99 (Statistical Parametric Mapping 99, the Wellcome Department of Cognitive Neurology, London, UK) program (Friston et al., 1995). Voxels with a P value of less than 0.05, corrected for multiple comparisons using distributional approximations from the Gaussian random field theory, were considered to have a significant difference (Worsley et al., 1992; Friston et al., 1994).

Results

In experiments I and II, there was no measurable difference between the sinograms of the transmission scans under TMS-on, TMS-off, and post-TMS conditions for any distance or orientation. Images acquired during TMS at a frequency of 5 Hz and an intensity of 80% of the maximum output of the TMS stimulator are shown in Fig. 3 (6 cm between edge of PET gantry and coil in parallel position) and Fig. 4 (2 cm between edge of PET gantry and coil in perpendicular position). In both figures, the central five sinograms of the transmission scans acquired in the TMS-on, TMS-off, and post-TMS conditions are laid on the first three rows (A–C), respectively. These sinograms and 2D subtraction images of the sinograms did not show any difference on visual inspection.

In Figs. 3 and 4, surface plots of the middle planes in (A–C) and their subtraction images are shown in (D) and (E) to allow a detailed inspection of the differences in the 2D images previously undetected. As shown in these images, no difference was found between the sinograms of the transmission scans. What is shown in Fig. 3E as a shadow does not present the difference between two images. It seems like a shadow since there is less count fluctuation in this region than the outside. The photon count under the coil

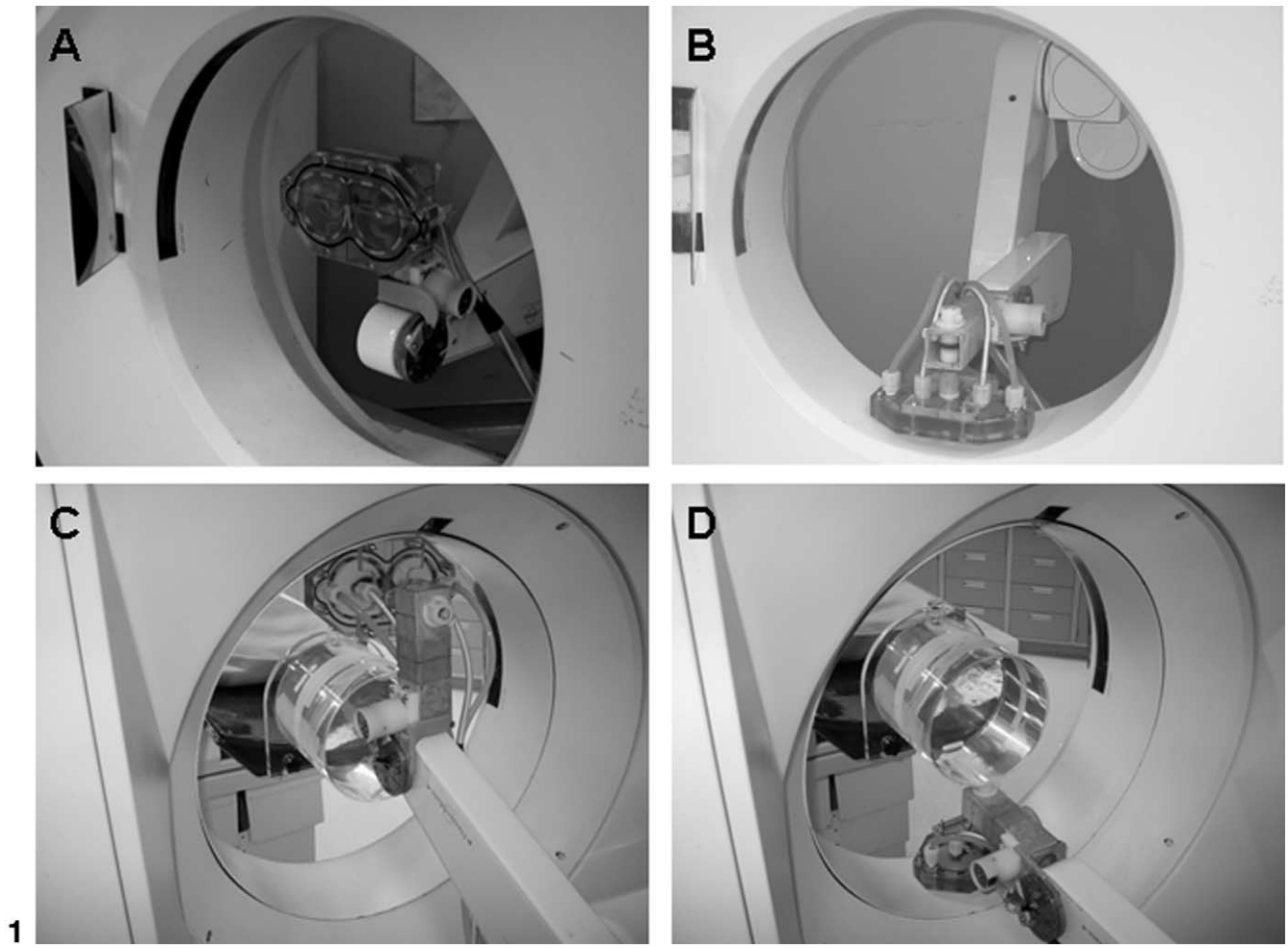

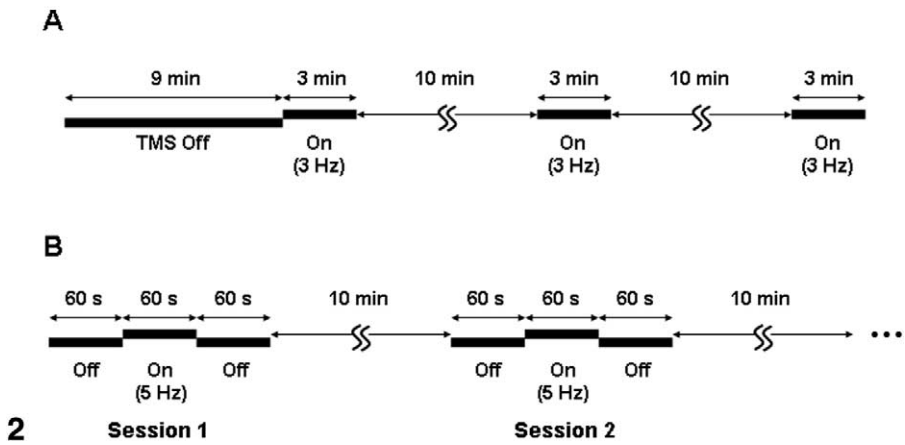

Fig. 1. Configuration of the TMS coil in the PET scanner. (A) Configuration of the maximum field of the TMS coil in the parallel orientation during experiments I and II. (B) Configuration of the maximum field of the TMS coil in the perpendicular orientation during experiments I and II. (C) Configuration of the maximum field of the TMS coil in the parallel orientation during experiment III. (D) Configuration of the maximum field of the TMS coil in the perpendicular orientation during experiment III.

Fig. 2. PET scan protocol. (A) Scan protocol used in experiment I: A 9-min transmission scan acquired during TMS-off condition followed by three TMS-on transmission scans of 3-min duration each acquired 10 min apart. (B) Scan protocol used in experiments II and III: nine sessions of transmission (experiment II) or emission (experiment III) scans were acquired. Each 3-min session consisted of a 1-min scan of TMS-off, TMS-on, and post-TMS conditions.

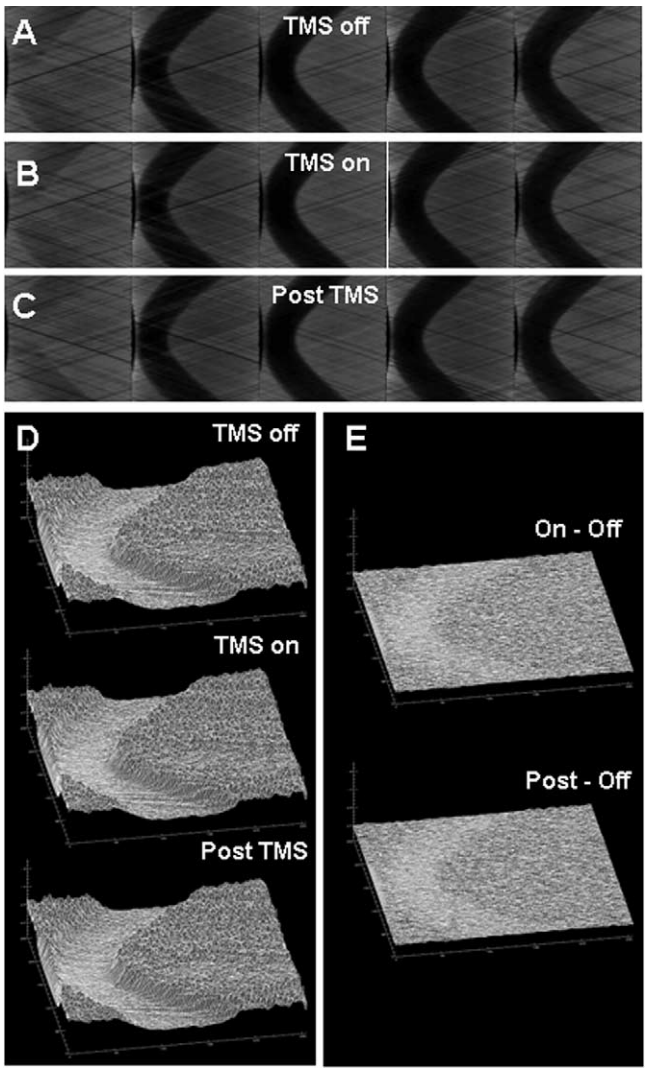

Fig. 3. Sinograms of the transmission scans with the maximum field of the TMS coil in the parallel orientation and 6 cm away from the edge of the PET gantry (experiment II, 5 Hz and 80% of maximum output of the stimulator). (A) TMS-off condition. (B) TMS-on condition. (C) Post-TMS condition. (D) Surface plot of the transmission scans during TMS-off, TMS-on, and post-TMS conditions. (E) Surface plot of subtraction images of the transmission scans shown in (D). Subtraction of TMS-on and TMS-off and subtraction of post-TMS and TMS-off are shown.

is lower than outside because of the attenuation. Therefore the difference in count in this region is small and its variation is also small according to the Poisson statistics.

No differences were detected between the reconstructed images of emission scans obtained in experiment III, as shown in Fig. 5 and 6, each of which shows the resulting images acquired in the parallel and perpendicular coil positions, respectively. In both figures, the central five reconstructed images of the emission scans acquired in each condition are laid on the first three rows (A–C). These images and surface plots of the middle planes (D) and their subtraction images (E) showed no differences between the TMS-off and the TMS-on/post-TMS conditions.

In addition, no statistically significant difference was found between any pair of conditions when the significance of each voxel was estimated at a threshold of $P = 0.05$ (corrected) using SPM software.

Discussion and conclusion

TMS is a method for the noninvasive stimulation of the cerebral cortex. Since TMS makes it possible to induce a focal current in the brain and transiently modulate the function of the targeted cortex, it has been used to study the electrophysiological response of a stimulated region, to treat

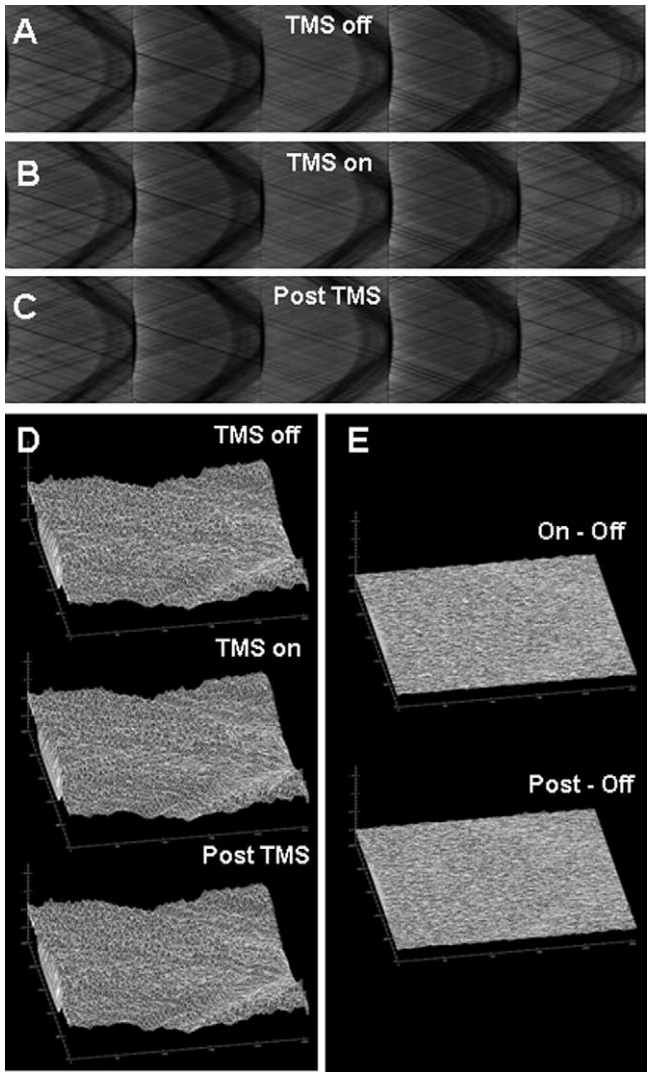

Fig. 4. Sinograms of the transmission scans with the maximum field of the TMS coil in the perpendicular orientation and 2 cm away from the edge of the PET gantry (experiment II, 5 Hz and 80% of maximum output of the stimulator). (A) TMS-off condition. (B) TMS-on condition. (C) Post-TMS condition. (D) Surface plot of the transmission scans during TMS-off, TMS-on, and post-TMS conditions. (E) Surface plot of the subtraction images of the transmission scans shown in (D). Subtraction of TMS-on and TMS-off and subtraction of post-TMS and TMS-off are shown.

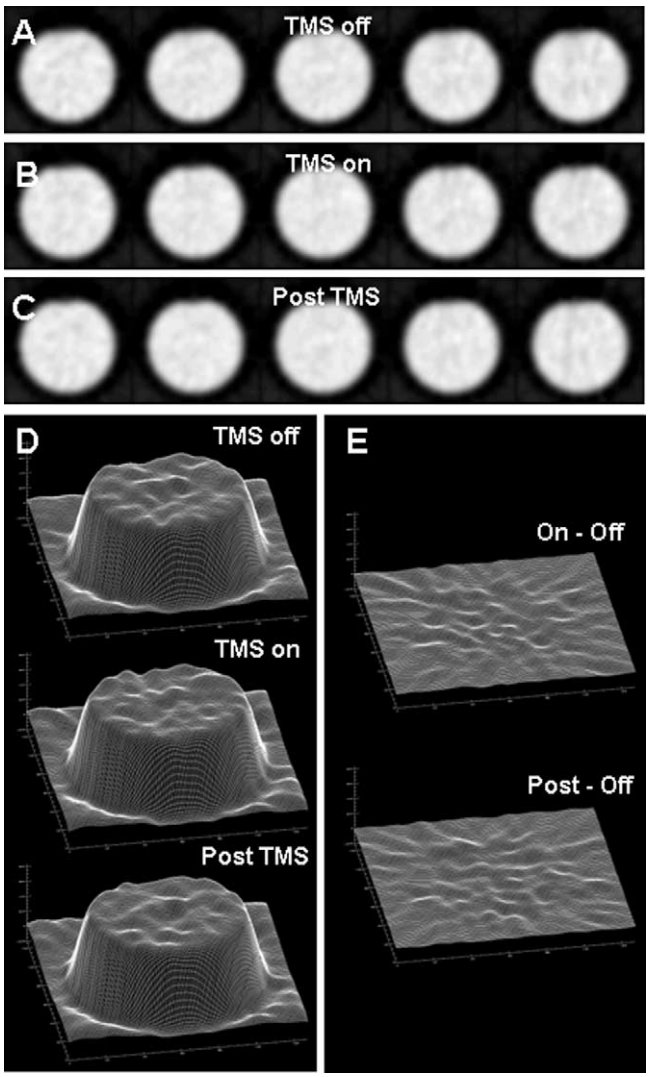

Fig. 5. Reconstructed images of the emission scans with the maximum field of the TMS coil in the parallel orientation and 6 cm away from the edge of the PET gantry (experiment III, 5 Hz and 80% of maximum output of the stimulator). (A) TMS-off condition. (B) TMS-on condition. (C) Post-TMS condition. (D) Surface plot of the emission scans during TMS-off, TMS-on, and post-TMS conditions. (E) Surface plot of subtraction images of the emission scans shown in (D). Subtraction of TMS-on and TMS-off and subtraction of post-TMS and TMS-off are shown.

patients with targeted repetitive stimulation, and to disturb ongoing neuronal pathways. Repetitive TMS (rTMS), which became available from 1987 onward, has resulted in a number of exciting new possible applications of magnetic stimulation. One of these is leading to novel approaches in functional brain mapping with PET (Fox et al., 1997; Paus et al., 1997, 1998), functional magnetic resonance imaging (fMRI) (Bohning et al., 1997, 1998), and electroencephalography (EEG) (Amassian et al., 1992; Ilmoniemi et al., 1997, 1999; Schurmann et al., 2001; Paus et al., 2001).

TMS/EEG is limited to showing effects in cerebral cortex and poses significant challenges in acquiring artifact-free data during TMS. The combination of TMS within PET or fMRI detects TMS-induced changes occurring anywhere in the brain and at high spatial resolution. Although fMRI is more widely available than PET, there are technical difficulties such as accessing the fMRI environment with TMS equipment, the possibility of damaging the stimulating coil, and the production of artifacts in fMRI images by magnetic field interactions. Thus, PET has been the imaging modality most widely used in combination with TMS.

For the above reason, the possible disturbance in the performance of PMTs used in a PET scanner by the rapidly changing magnetic fields (1–2 T) induced by TMS are a major concern. Magnetic fields can alter the electron trajec-

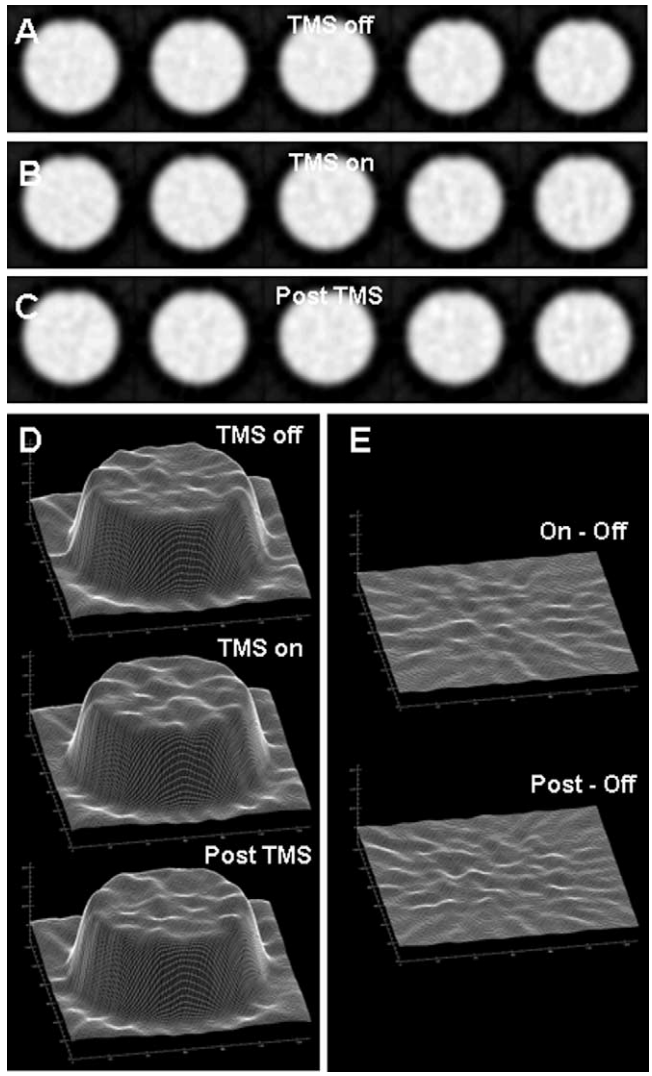

Fig. 6. Reconstructed images of the emission scans with the maximum field of the TMS coil in the a perpendicular position and 2 cm away from the edge of the PET gantry (experiment III, 5 Hz and 80% of maximum output of the stimulator). (A) TMS-off condition. (B) TMS-on condition. (C) Post-TMS condition. (D) Surface plot of the emission scans during TMS-off, TMS-on, and post-TMS conditions. (E) Surface plot of the subtraction images of the emission scans shown in (D). Subtraction of TMS-on and TMS-off and subtraction of post-TMS and TMS-off are shown.

tories from photocathode and dynodes in the PMTs and cause variations in the sensitivity of PMTs (Paus et al., 1997; Thompson et al., 1998; Paus, 1999). For this reason, Thompson and colleagues examined the effect of magnetic field on PET detectors using a single detector assembly before initiating their combined TMS/PET studies and suggested the placement of 3–4 sheets of well-grounded μ-metal between the coil and the PET detector to minimize the effect of the magnetic field by TMS (Thompson et al., 1998). Their observation, however, was contrary to the report by Fox et al. who imaged a line phantom with ^{18}F and did not find any difference between the TMS-on and TMS-off conditions (Fox et al., 1997).

In the current study, extensive experiments with various possible conditions were performed to determine whether the TMS discharging during PET affects its image quality. Qualitative and quantitative evaluation of the transmission and emission PET scans indicated no measurable difference between the TMS-on and -off conditions, even with rigorous levels of TMS. Moreover, no posteffects of the magnetic field on PET data acquisition were evident.

Findings from two other groups that have also examined the effect of TMS on PET scanners support our results. Bruce Weber and Alfred Buck at the University Hospital, Zurich (personal communication), have tested effects of TMS on a GE Advance PET scanner. The data were acquired in the 3D mode. In the first experiment, using a Magstim Standard Rapid Stimulator (Magstim Company Ltd., Spring Gardens, Wales UK) with an air-cooled B-shape coil, discharging at 3 Hz and 70% of max stimulator output, they acquired four 60-s emission scans of FDG phantoms during both TMS-on and TMS-off conditions. The coil was held perpendicular to the longitudinal axis of the PET scanner. SPM analyses of the FDG phantom images acquired during TMS-on and TMS-off conditions did not find any significant difference between the two conditions. In the second experiment, blank scans were acquired during TMS-on and TMS-off conditions using the same specifications as in experiment I. No obvious dropouts were detected on the sinograms. However, this finding was not verified statistically. This group has performed numerous TMS-PET experiments without μ-metal shielding and has not reported any TMS-induced artifacts.

Margaret Daube-Witherspoon (personal communication), at the University of Pennsylvania, also made measurements with Magstim Super Rapid Magnetic Stimulator with an air-cooled B-shape coil in the GE Advance PET scanner and found no effect on spatial resolution or uniformity. The TMS paddle was placed at a location where it would be used on humans (i.e., not at the edge of the patient aperture, close to the detectors), and phantom studies were performed. The conclusion from these experiments was that were no measurable effects of the magnetic stimulation, even at the maximum stimulator output, for either 1- or 20-Hz frequencies, and that μ-metal shielding was not required.

The lack of an effect of TMS on PET data acquisition can be explained in two ways. First, the distance between the TMS coil and the detector block in the PET scanner is great enough to significantly reduce the magnetic field. The field falls off in proportion to the square of distance (3% of maximum field at 10 cm in air). Since long interplane septal collimators are placed between the detector module and the patient port of the gantry, the PET detector is about 10–20 cm away from the coil in all currently available dedicated PET scanners. For example, the distance between the detector ring and the patient port of gantry of the scanner used in this study (GE 4096) is 22 cm, and that of CTI ECAT EXACT is 13.1 cm (detector ring diameter: 82.4 cm, patient port diameter: 56.2 cm). Second, the duration of the TMS pulses is very short relative to the total PET acquisition time. The duration of a single TMS pulse is 200–250 μs. Even if we assume the magnetic field affects the operation of PMT, and the TMS stimulation frequency is 10 Hz, its effective time is only 0.2–0.25% of total PET acquisition time. This means that only 2 or 3 photons of 1000 photons detected by the PET detector will be affected by the field, assuming no posteffect of the magnetic field. This effect is very small relative to the statistical and electronic noise of the photon detection.

The results of this study, in which the experiments were more appropriately performed inside the PET, rather than in isolated detectors, contradict Thompson's report (Thompson et al., 1998). However, they looked only for changes in the detector output, which could be well below the level necessary to affect the sinograms and the reconstructed image. The effects observed by Thompson et al. could also have been due to other metal in the environment creating induced currents, which would not be present in PET.

We conclude that μ-metal shielding of a PET scanner during TMS is not necessary at least in the two PET scanners tested to date and is unlikely to be necessary in any PET scanner. We advise against the use of μ-metal shield as a "better safe than sorry" precautionary measure, because the increased attenuation from the shielding reduces coincidence counts by 22% (Paus et al., 1997). It is important to realize that the scatter caused by the μ-metal shielding in the FOV not only reduces the total true coincidence counts, but also results in increased false localization of the anihilation event. The errors in localization become important especially in a 3D acquisition mode. For ^{15}O-water studies, loss of counts can be overcome only by increasing the injected dose and, therefore, increasing subject risk. We recommend that laboratories using PET cameras other than those described here or TMS stimulation protocols different than those reported here test scanner performance as we have done and use μ-metal shielding only if scanner performance is *better* in the shielded environment than the unshielded.

Acknowledgments

This work was supported in part by National Institute of Mental Health Grant R01-MH60246 awarded to Dr. Fox and in part by the Korean Ministry of Science and Technology. Dr. Jae Sung Lee's stay at the Research Imaging Center was funded by the International Atomic Energy Agency.

References

Amassian, V.E., Cracco, R.Q., Maccabee, P.J., Cracco, J.B., 1992. Cerebello-frontal cortical projections in humans studied with the magnetic coil. Electroencephalogr. Clin. Neurophysiol. 85, 265–272.

Barker, A.T., Jalinous, R., Freeston, I.L., 1985. Non-invasive magnetic stimulation of the motor cortex. Lancet 1, 1106–1107.

Bohning, D.E., Pecheny, A.P., Epstein, C.M., Speer, A.M., Vincent, D.J., Dannels, W., George, M.S., 1997. Mapping transcranial magnetic stimulation (TMS) fields in vivo with MRI. NeuroReport 8, 2535–2538.

Bohning, D.E., Shastri, A., Nahas, Z., Lorberbaum, J.P., Andersen, S.W., Dannels, W.R., Haxthausen, E.U., Vincent, D.J., George, M.S., 1998. Echoplanar BOLD fMRI of brain activation induced by concurrent transcranial magnetic stimulation. Invest. Radiol. 33, 336–340.

Fox, P., Ingham, R., George, M.S., Mayberg, H., Ingham, J., Roby, J., Martin, C., Jerabek, P., 1997. Imaging human intra-cerebral connectivity by PET during TMS. NeuroReport 8, 2787–2791.

Friston, K.J., Worsley, K.J., Frackowiak, R.S.J., Mazziotta, J.C., Evans, A.C., 1994. Assessing the significance of focal activations using their spatial extent. Hum. Brain Mapp. 1, 210–220.

Friston, K.J., Holmes, A.P., Worsley, K.J., Poline, J-P., Frith, C.D., Frackowiak, R.S.J., 1995. Statistical parametric maps in functional imaging: a general linear approach. Hum. Brain Mapp. 2, 189–210.

Fox, P., Ingham, R., George, M.S., Mayberg, H., Ingham, J., Roby, J., Martin, C., Jerabek, P., 1997. Imaging human intra-cerebral connectivity by PET during TMS. NeuroReport 8, 2787–2791.

Ilmoniemi, R.J., Virtanen, J., Ruohonen, J., Karhu, J., Aronen, H.J., Naatanen, R., Katila, T., 1997. Neuronal responses to magnetic stimulation reveal cortical reactivity and connectivity. NeuroReport 8, 3537–3540.

Ilmoniemi, R.J., Ruohonen, J., Karhu, J., 1999. Transcranial magnetic stimulation—a new tool for functional imaging of the brain. Crit. Rev. Biomed. Eng. 27, 241–284.

Lee, J.S., Kim, K.M., Lee, D.S., Paek, M.Y., Ahn, J.Y., Paus, T., Park, K.S., Chung, J-K., Lee, M.C., 2000. Significant effect of subject movement during brain PET imaging with transcranial magnetic stimulation. J. Nucl. Med. 41, 186P [Abstract].

Narayana, S., Fox, P.T., Tandon, N., Lancaster, J.L., Roby III, J., Constantine, W., 2000. Use of neurosurgical robot for aiming and holding in cortical TMS experiments. NeuroImage 11, S471 [Abstract].

Narayana, S., Fox, P.T., Tandon, N., Franklin, C., Cervantes, G., Lancaster, J.L., June 2002. Primary motor cortical response to alterations in TMS intensity: a PET-EMG comparative analysis. NeuroImage 16, Abstract 556.

Pascual-Leone, A., Walsh, V., 2002. Transcranial magnetic stimulation, in: Toga, A.W, Maziotta, J.C. (Eds.), Brain Mapping: The methods, 2nd ed., Academic Press, San Diego, pp. 255–290.

Paus, T., Jech, R., Thompson, C.J., Comeau, R., Peters, T., Evans, A.C., 1997. Transcranial magnetic stimulation during positron emission tomography: a new method for studying connectivity of the human cerebral cortex. J. Neurosci. 17, 3178–3184.

Paus, T., Jech, R., Thompson, C.J., Comeau, R., Peters, T., Evans, A.C., 1998. Dose-dependent reduction of cerebral blood flow during rapid-rate transcranial magnetic stimulation of the human sensorimotor cortex. J. Neurophysiol. 79, 1102–1107.

Paus, T., 1999. Imaging the brain before, during, and after transcranial magnetic stimulation. Neuropsychologia 37, 219–224.

Paus, T., Sipila, P.K., Strafella, A.P., 2001. Synchronization of neuronal activity in the human primary motor cortex by transcranial magnetic stimulation: an EEG study. J. Neurophysiol. 86 (4), 1983–1990.

Schurmann, M., Nikouline, V.V., Soljanlahti, S., Ollikainen, M., Basar, E., Ilmoniemi, R.J., 2001. EEG responses to combined somatosensory and transcranial magnetic stimulation. Clin. Neurophysiol. 112, 19–24.

Tandon, N., Narayana, S., Zamarripa, F., Lancaster, J.L., and Fox, P.T., June 2001. Transcranial magnetic stimulation (TMS) intensity dependent alterations in regional cerebral blood flow. NeuroImage 13(6) S1010. [Abstract].

Thompson, C.J., Paus, T., Clancy, R., 1998. Magnetic shielding requirements for PET detectors during transcranial magnetic stimulation. IEEE Trans. Nucl. Sci. 45, 1303–1307.

Worsley, K.J., Evans, A.C., Marrett, S., Neelin, P., 1992. A three-dimensional statistical analysis for CBF activation studies in human brain. J. Cereb. Blood Flow Metab. 12, 900–918.